RESEARCH ARTICLE

American Society of Plant Biologists | SOCIETY FOR EXPERIMENTAL BIOLOGY | WILEY

PELOTA and HBS1 suppress co-translational messenger RNA decay in Arabidopsis

Rong Guo | Brian D. Gregory

Department of Biology, University of Pennsylvania, Philadelphia, PA, USA

Correspondence
Brian D. Gregory, Department of Biology, University of Pennsylvania, 433 S. University Ave., Philadelphia, PA 19104.
Email: bdgregor@sas.upenn.edu

Abstract

Various messenger RNA (mRNA) decay mechanisms play major roles in controlling mRNA quality and quantity in eukaryotic organisms under different conditions. While it is known that the recently discovered co-translational mRNA decay (CTRD), the mechanism that allows mRNAs to be degraded while still being actively translated, is prevalent in yeast, humans, and various angiosperms, the regulation of this decay mechanism is less well studied. Moreover, it is still unclear whether this decay mechanism plays any role in the regulation of specific physiological processes in eukaryotes. Here, by re-analyzing the publicly available polysome profiling or ribosome footprinting and degradome sequencing datasets, we discovered that highly translated mRNAs tend to have lower co-translational decay levels. Based on this finding, we then identified Pelota and Hbs1, the translation-related ribosome rescue factors, as suppressors of co-translational mRNA decay in Arabidopsis. Furthermore, we found that Pelota and Hbs1 null mutants have lower germination rates compared to the wild-type plants, implying that proper regulation of co-translational mRNA decay is essential for normal developmental processes. In total, our study provides further insights into the regulation of CTRD in Arabidopsis and demonstrates that this decay mechanism does play important roles in Arabidopsis physiological processes.

1 | INTRODUCTION

mRNA quality and quantity must be tightly controlled to ensure the normal functions of eukaryotic organisms during different growth stages and in response to varying environments. While this control largely relies on processes such as mRNA transcription and pre-mRNA processing, it is also largely dependent on mRNA degradation. In eukaryotes, mRNA degradation can be initiated both endonucleolytically or exonucleolytically. Endonucleolytic mRNA cleavage can be done via microRNA (miRNA)- and small interfering RNA (siRNA)-mediated RNA interference, or simply by various endonucleases (Heck & Wilusz, 2018; Park & Shin, 2014). Exonucleolytic mRNA decay generally begins with the shortening or removal of the polyadenine (polyA) tail, a process referred to as deadenylation. Following deadenylation, the mRNA can be degraded 3' to 5' by the exosome complex. Alternatively, the mRNA can subsequently undergo cap removal and then be degraded 5' to 3' by various exonuclease (Belostotsky & Sieburth, 2009; Nagarajan et al., 2013).

Although it was once believed that mRNA decay only occurs after the translation process has been completed, cumulative evidence suggested that decay can also occur directly in translating mRNAs (Heck & Wilusz, 2018; Parker, 2012). In support of eukaryotic co-translational mRNA decay (CTRD), it was previously discovered in yeast that decapped mRNAs are purified in the polysome fractions,

---

suggesting that decay was actually occurring on translating mRNAs (Hu et al., 2009, 2010). Subsequently, using various degradome sequencing techniques such as genome-wide mapping of uncapped and cleaved transcripts (GMUCT), parallel analysis of RNA ends (PARE-seq), and Akron5-Seq, all of which capture and sequence the mRNA degradation intermediates bearing a monophosphate group at their 5′ ends (Addo-Quaye et al., 2008; German et al., 2009; Gregory et al., 2008; Ibrahim et al., 2018), different groups found that co-translational mRNA decay is conserved not only in the yeast species *Saccharomyces cerevisiae* and *Saccharomyces pombe*, but also in at least 10 angiosperms as well as in human transcriptomes (Addo-Quaye et al., 2008; German et al., 2009; Gregory et al., 2008; Guo et al., 2023; Ibrahim et al., 2018). Specifically, a three-nucleotide periodicity of 5′ P read ends was revealed along the mRNA open reading frames (ORFs) using sequencing reads from these approaches. This pattern is generated by the exonuclease responsible for CTRD cleaving immediately upstream of the trailing edge of translating ribosomes that move in three nucleotide intervals. Furthermore, the 5′ P read ends of CTRD mRNAs have also been shown to accumulate 16 to 17 nucleotides (nt) upstream of the stop codon, suggesting that ribosomes pause longer at stop codons when translation terminates (Guo et al., 2023; Hou et al., 2016; Ibrahim et al., 2018; Pelechano et al., 2015; Yu et al., 2016).

Despite the prevalence of co-translational mRNA decay in multiple organisms, its regulation and physiological roles are relatively less studied. Although analysis of sequence features of the CTRD mRNAs in angiosperms showed that the mRNAs degraded by this pathway generally possess sequence features associated with low translation efficiency, it is still not understood whether and how co-translational mRNA decay and translation efficiency are actually connected (Guo et al., 2023). Current knowledge in co-translational mRNA decay-regulating factors is also somewhat limited. It has only been revealed that Arabidopsis exonuclease XRN4 (XRN1 in yeast) is required for co-translational mRNA decay and Arabidopsis CBP80/ABH1 also has an impact on this pathway (Pelechano et al., 2015; Yu et al., 2016). However, aside from these two factors, it is not known if there are any other factors that play roles in regulating CTRD. Moreover, it is unclear if there are any proteins that act as suppressors of this decay pathway.

The only confirmed physiological role of CTRD is in the autoregulation of tubulin in mammalian cells. In the presence of excess soluble tubulin, tetratricopeptide protein 5 (TTC5) interacts with both the ribosome and the nascent tubulin peptide to trigger CTRD of the tubulin mRNA, which decreases the total amount of tubulin mRNA and maintains the overall abundance of soluble tubulin in the cell (Lin et al., 2020). In plants, although it is known that CTRD is widespread across different growth stages and environmental conditions in at least 10 angiosperms (Guo et al., 2023), it is not known what role this decay pathway plays in the different physiological processes involved in normal plant development and various environmental responses.

Pelota (Dom34 in yeast) and Hbs1 are ribosome-rescuing factors responsible for recycling ribosomes that are stalled at the end of stop-codon-less mRNAs or in the middle of CDS in mammals and yeast (Hilal et al., 2016; Pisareva et al., 2011; Tsuboi et al., 2012). Meanwhile, the loss of Dom34 in yeast also results in ribosome

accumulation in the 3′ UTR of numerous mRNAs in vivo (Guydosh & Green, 2014). While the homologs of yeast and human Pelota and Hbs1 have been identified in Arabidopsis (Kong et al., 2021; Zhang et al., 2018), their molecular functions are not comprehensively studied compared to their counterpart in humans and yeast. Currently, it has only been shown from agroinfiltration experiments in tobacco leaves that both Arabidopsis Pelota and Hbs1 are essential in the degradation of stop codon-less reporter transcripts or those with long stretches of adenines in their coding regions (Szádeczky-Kardoss et al., 2018, 2018). However, the molecular functions of Arabidopsis Pelota and Hbs1 *in planta* are still unclear. Also, whether they can function in co-translational mRNA decay has never been studied.

In this study, by re-analyzing the publicly available high-quality polysome profiling or ribosome footprinting, mRNA-seq, and GMUCT datasets available for Arabidopsis, we found that the co-translational decay level and translation efficiency are in general inversely related to each other, suggesting that translation efficiency does play some roles in co-translational mRNA decay. Using GMUCT, we then revealed that Arabidopsis Pelota and Hbs1, the two factors known to function as ribosome rescuing factors in tobacco leaves (Szádeczky-Kardoss et al., 2018, 2018) and in vivo in other metazoans (Hilal et al., 2016; Pisareva et al., 2011; Tsuboi et al., 2012), are able to suppress co-translational mRNA decay *in planta*. Finally, we explored if co-translational mRNA decay functions in any physiological processes by assessing the phenotypes of Pelota and Hbs1 null mutants (*pel1–1, pel1–2, hbs1–1,* and *hbs1–2*) and found that these mutant plants display lower germination rates compared to the wild type plants, suggesting that mis-regulated co-translational mRNA decay can lead to negative physiological outcomes in Arabidopsis.

Taken together, our study reveals the relationship between translation efficiency and co-translational decay levels, which provides additional directions for the study of the initiation mechanisms of co-translational mRNA decay. We have also identified two suppressors of CTRD in plants, indicating that co-translational mRNA decay is a complex and tightly regulated process that has not been studied widely enough. Lastly, we demonstrated that proper regulation of co-translational decay is essential for normal physiological functions in Arabidopsis.

2 | RESULTS

2.1 | CTRD level is inversely related to translation efficiency in Arabidopsis mRNAs

We previously reported that in angiosperm transcriptomes mRNAs degraded by the CTRD mechanism generally harbor sequence features such as longer 5′ UTR, longer CDSs, and higher 5′ UTR GC content that are associated with low translation efficiency. Meanwhile, these mRNAs are also enriched with codons that could slow down ribosomes directly or encode amino acids that cause increased ribosome stalling, which are likely to further result in overall slower ribosome elongation (Guo et al., 2023). Given the presence of this low

translation activity favoring sequence features in co-translationally decayed mRNAs, we wondered whether the CTRD level of mRNAs is related to their translation level in Arabidopsis.

According to our previous study, the CTRD levels of a specific mRNA species is best represented by the Terminal Stalling Index (TSI), which is calculated using degradome sequencing reads. Specifically, the TSI is calculated by dividing the average number of 5' P read ends that accumulate at the 5′ ribosome boundary of the translation termination sites (16 and 17 nt upstream of the first nucleotide of the stop codon) by the average number of 5' P read ends that accumulate within the entire 100 nt flanking regions of the first nucleotide of the stop codon (Guo et al., 2023). Since TSI directly reflects the level of 5' P read ends that accumulate at the 5′ ribosome boundary of translation termination sites, higher TSI values mean higher CTRD levels for a specific mRNA species.

Aside from the 5' P read end accumulation at the 5′ ribosome boundary of translation termination sites, the strength of the three-nucleotide periodicity present in degradome sequencing datasets can also be employed as a proxy for the level of CTRD (Pelechano et al., 2015; Yu et al., 2016). In Arabidopsis, the three-nucleotide periodicity strength was measured using the co-translational RNA decay index (CRI), which is defined as the $\log_2$ ratio of the average 5' read end counts in the two reading frames (frames 1 and 2) that are cleaved more frequently by XRN4 to the 5′ read end count in the reading frame that is protected by the ribosome (frame 0) (Yu et al., 2016). Furthermore, the CRI value is also positively correlated with the TSI value (Supplemental Figure 1C). In fact, higher CRI values correspond to higher CTRD levels for a specific mRNA species. However, since CRI is not as robust as TSI (Guo et al., 2023), we use TSI as the primary proxy to determine which mRNAs undergo CTRD as well as measure the level of CTRD while only using CRI as a supplemental method for measuring the level of CTRD.

The translation level of a specific mRNA species is commonly estimated by assessing the number of mRNAs associated with translating ribosomes, which can be measured by either polysome profiling or ribosome footprinting (Dermit et al., 2017). For polysome profiling, the polysomes are purified by sedimentation in a sucrose gradient and the polysome-associated mRNAs are then quantified by RNA sequencing (Arava et al., 2003; Karginov & Hannon, 2013). In ribosome footprinting, the ribosome-protected fragments (RPFs) are isolated after mild RNase digestion and subsequently analyzed by RNA sequencing (Ingolia et al., 2009; Piccirillo et al., 2014). In order to account for the translational differences caused by changes in the level of RNA abundance for a given mRNA species, the count obtained from polysome or RPF libraries is normalized to the count obtained from total RNA sequencing libraries prepared in parallel. The result is defined as translation efficiency for the mRNA species (Ingolia et al., 2009), the higher the translation efficiency the more the mRNA species is translated.

To address the question above, we gathered publicly available high-quality Arabidopsis degradome sequencing datasets along with their matching polysome profiling or ribosome footprinting datasets and mRNA-seq datasets from the GEO database (Carpentier

et al., 2020; Lin et al., 2017; Liu et al., 2013), from which the TSI values as well as the translation efficiency for each transcript were calculated. As done before, the mRNAs with TSI values higher than three were considered to be those that are CTRD mRNAs and used in subsequent analyses (Guo et al., 2023). The co-translationally decayed mRNAs were then separated into high translation efficiency or low translation efficiency groups if their translation efficiency value fell within the top 34% or bottom 34%, respectively, among all co-translationally decayed mRNAs.

In four out of the five datasets analyzed, we observed that the median TSI value of the co-translationally decayed mRNAs with higher translation efficiency is significantly lower compared to that of the co-translationally decayed mRNAs with lower translation efficiency (Figure 1a; all p-values < .05; Wilcoxon signed rank test), indicating that the highly translated mRNAs have an overall lower co-translational decay level. A dataset generated from 25-day-old seedlings was the only outlier, in which no significant difference in median TSI was observed between co-translationally decayed mRNAs with higher translation efficiency and those with lower translation efficiency (Figure 1a, bottom right panel). The same results were obtained when using CRI as the co-translational mRNA decay level proxy— mRNAs in the high translation efficiency group have significantly lower median CRI compared to those in the low translation efficiency group in all the datasets except for that generated from 25-day-old seedlings, in which no significant difference in median CRI between the two groups of mRNAs was observed (Supplemental Figure 1A,B; all p-values < .05; Wilcoxon signed-rank test).

Since the inverse relationship between co-translational decay level and translation efficiency of mRNAs can be observed in 80% of the datasets analyzed, we conclude that in general transcripts with a higher translation level generally have lower CTRD levels, which further implies that translation level is a major determinant in how much an mRNA undergoes CTRD.

2.2 | Translation-related ribosome rescue factors Pelota and Hbs1 suppress co-translational mRNA decay in vivo in Arabidopsis

Given the observation that lesser translated mRNAs have a higher level of CTRD (Figure 1 and Supplemental Figure 1) and that translation level is related to ribosome behavior, we next explored if factors that are able to impact ribosome behavior can also regulate co-translational mRNA decay. It was found that yeast and mammalian Pelota and Hbs1 are able to rescue ribosomes that are stalled at the end of stop-codon-less transcripts or in the middle of CDS in vitro while loss of Pelota or Hbs1 in vivo results in changes in ribosome behaviors (Guydosh & Green, 2014; Pisareva et al., 2011; Tsuboi et al., 2012). Although it is known that the Arabidopsis Pelota and Hbs1 also function in tobacco leaves by dissociating stalled ribosomes (Szádeczky-Kardoss et al., 2018, 2018), their molecular functions in Arabidopsis have not been well studied. Therefore, we wondered if Pelota and Hbs1 can regulate CTRD in Arabidopsis.
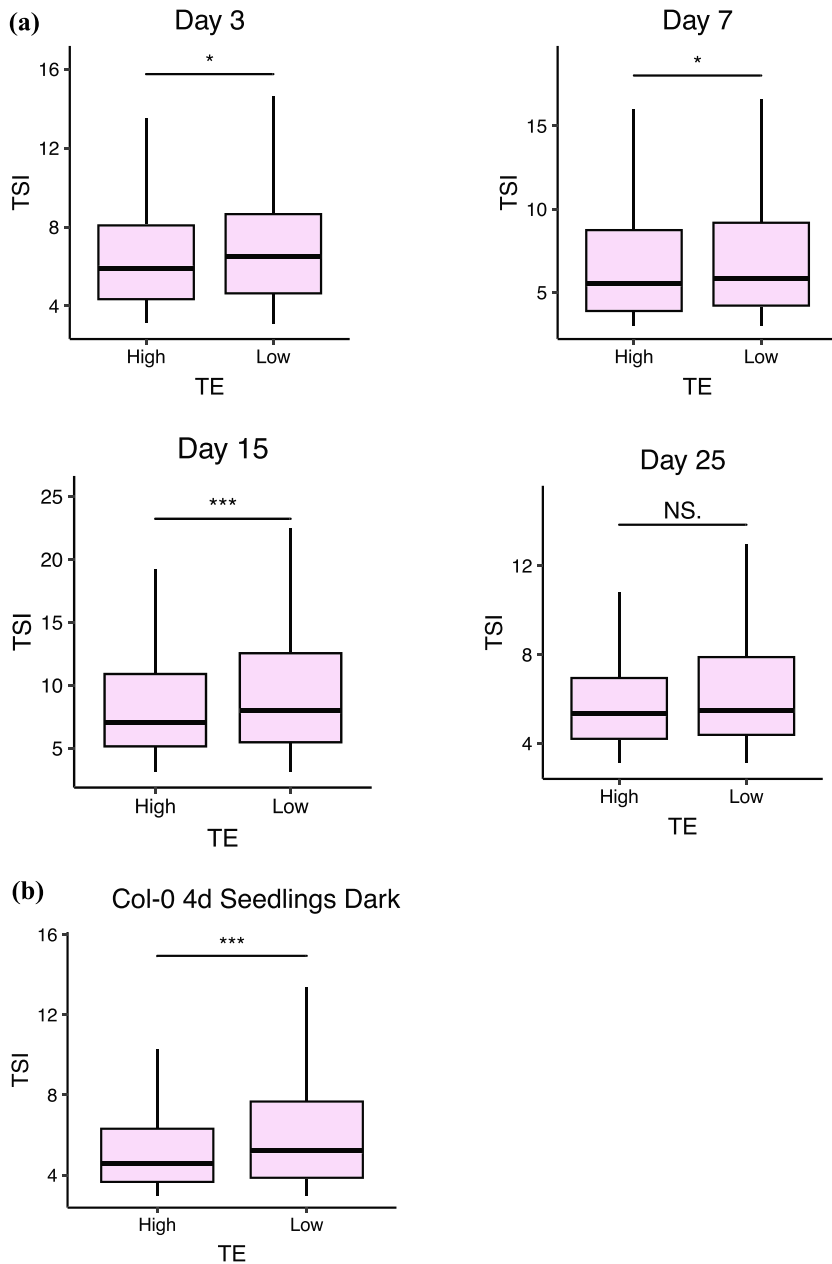
**FIGURE 1** Co-translational decay level is inversely related to the translation level. Transcripts with higher translation efficiency generally have lower TSI (and vice versa) in (a) three-day-old, seven-day-old, 15-day-old, and 25-day-old Arabidopsis seedlings grown under regular growth conditions and (b) four-day-old Arabidopsis seedlings grown in dark conditions. TSI indicates terminal stalling index while TE indicates translation efficiency. *** and * denote p-value < .001 and < .05, respectively, while NS denotes p-value > .05 as determined by Wilcoxon test.

To answer this question, we constructed GMUCT libraries in triplicate using 12-day-old seedlings of wild-type Col-0 plants as well as both Pelota (*pel1–1*; hereafter *pel*) and Hbs1 (*hbs1–1*; hereafter *hbs1*) null mutants. The libraries were sequenced with all generating ∼23–40 million mapped reads per library (Supplemental Table 1). The libraries from the biological replicates of each distinct genotype clustered together (Supplemental Figure 2A), indicating the high quality and reproducibility of these libraries. The sequencing results were analyzed using our previously established pipeline where mRNAs displaying TSI values greater than three are considered to be co-translationally decayed (Guo et al., 2023; Yu et al., 2016). We then assessed the status of CTRD in both of the null mutants and wild-type plants using two different measurements. We first compared the number of co-translationally decayed mRNAs identified in the null

mutants with the number of those identified in wild-type plants. In total, we identified 787 co-translationally decayed mRNAs in *pel*, 1,048 in *hbs1*, but only 690 in wild-type plants (Figure 2a). In other words, *pel* and *hbs1* mutant plants have 14% and 52% more co-translationally decayed mRNAs, respectively, compared to that in wild-type plants, indicating that loss of either Pelota or Hbs1 results in more mRNAs being decayed co-translationally, suggesting that both Pelota and Hbs1 are able to suppress CTRD *in planta*. The percentage increase in the number of co-translationally decayed mRNAs of *hbs1* is also much higher compared to that of *pel*, suggesting that Hbs1 has a stronger inhibitory effect on CTRD compared to Pelota.

To confirm that the CTRD level of the co-translationally decayed mRNAs truly increases in *pel* and *hbs1* mutant plants, we also calculated the CRI value for every identified co-translationally decayed

FIGURE 2 **Pelota and Hbs1 suppress CTRD in vivo.** (a) The number of mRNAs sorted into the co-translational decay pathway increased when knocking out Pelota or Hbs1. (b) Distribution of co-translational RNA decay index (CRI) indicates that knocking out Pelota or Hbs1 resulted in global increases of CRI among the collection of co-translationally decayed mRNAs. All the differences were found to be statistically significant with p-values < .05 as determined using Wilcoxon signed rank tests.
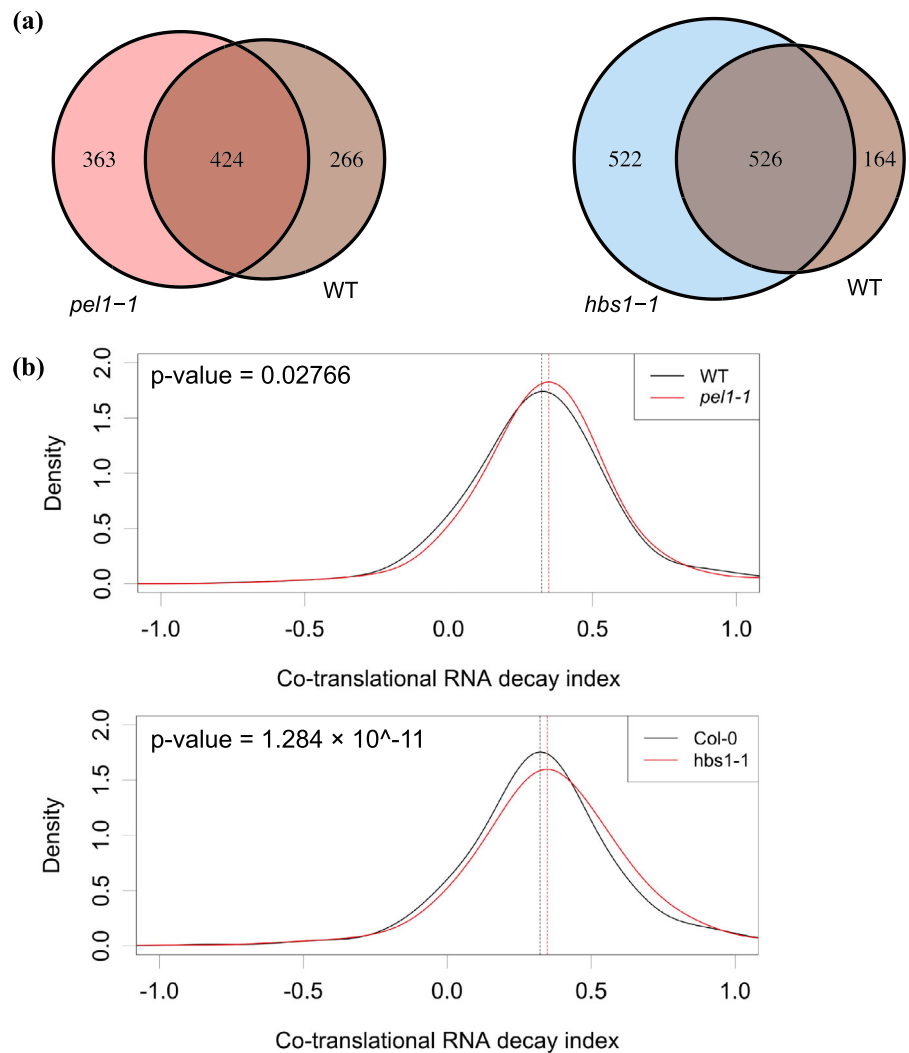

mRNA in the mutants and compared that with the CRI value in the wild-type plants. As expected, we found that the median of CRI distribution for co-translationally decayed mRNAs is significantly higher in both *pel* and *hbs1* mutant as compared to that in wild-type plants (Figure 2b; p-values < .05 and .001 in upper and bottom panels, respectively; Wilcoxon signed-rank test). Taken together, these results revealed that both Pelota and Hbs1 can repress CTRD in Arabidopsis, and between these two factors, Hbs1 has a greater impact on this decay pathway.

2.3 | Pelota and Hbs1 suppress the CTRD of a wide range of mRNAs encoding proteins with various functions

After discovering that both Pelota and Hbs1 can suppress CTRD, we then wondered if there are any specific functions associated with the mRNAs whose co-translational decay is suppressed by these two factors. To test this, we performed gene ontology analysis on the co-translationally decayed mRNAs that are specific to

either of the null mutants using agriGO (Tian et al., 2017). By analyzing the GO terms for biological processes, we found that this group of mRNAs in both null mutants are highly enriched in various GO terms ranging from development processes to stress response (Figure 3), indicating that both Pelota and Hbs1 are able to target mRNAs that encode proteins with various functions. Meanwhile, we observed more than 50% overlap between the analyzed GO terms in both *pel* and *hbs1* mutants (Supplemental Figure 3A), suggesting that the CTRD targets of Pelota and Hbs1 function in very similar processes.

Interestingly, early development-related GO terms such as post-embryonic morphogenesis as well as stress response-related GO terms such as cellular response to oxygen-containing compounds and response to light stimulus are highly enriched in the co-translationally decayed mRNAs of both null mutants (Figure 3), implying that CTRD suppression by Pelota and Hbs1 might be essential for these processes in Arabidopsis. In total, our results indicate that CTRD suppression by Pelota and Hbs1 is prevalent among mRNAs involved in various biological processes in plant transcriptomes.

(a)

(b)
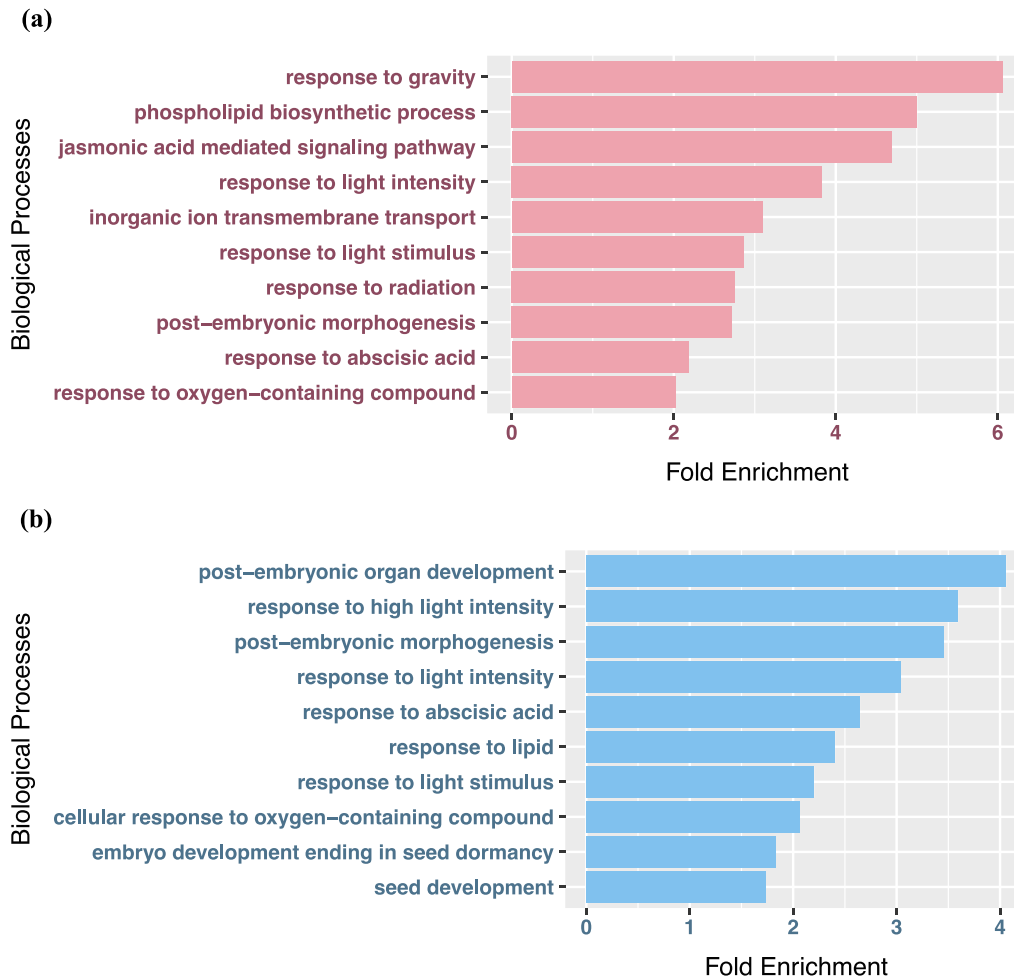
FIGURE 3 **Pelota and Hbs1 can suppress the co-translational decay of mRNAs with a wide range of functions.** Top gene ontology terms (biological processes) enriched from the co-translationally decayed mRNAs specific to (a) Pelota null mutants and (b) Hbs1 null mutants. The adjusted p-values of all terms presented are below .05. The fold enrichment was calculated by dividing the percentage of genes belonging to a certain term in the input list by the percentage of genes belonging to the same term in the background.

2.4 | Pelota and Hbs1 null mutants have lower germination rates compared to wild-type plants

We next asked if CTRD suppression is truly essential for Arabidopsis development and stress response. We reasoned that if the suppression of this pathway is essential, changes in phenotypes related to growth or stress response should be observed in both *pel* and *hbs1* mutant plants compared to wild type given that the CTRD of numerous mRNAs responsible for development and stress responses are not properly suppressed in these two mutant backgrounds. To analyze the growth-related phenotypes, we grew Pelota mutants (*pel1–1* and *pel1–2*), Hbs1 mutants (*hbs1–1* and *hbs1–2*), as well as wild-type plants under regular growth conditions and tracked their phenotypes on a daily basis. Two mutant alleles of each gene were used in order to rule out the possibility that the observed phenotypes are caused by unknown mutations existing in the plant backgrounds. Using protrusion of radicles as the sign of germination (Finch-Savage & Leubner-Metzger, 2006; Steinbrecher & Leubner-Metzger, 2017), we found that the final

germination rate of *pel1–1*, *pel1–2*, *hbs1–1*, and *hbs1–2* is significantly (all P < .01; Mann–Whitney U test) lower (62%, 40%, 40%, and 75%, respectively) than that of the wild type plants after seven days (Figure 4a,b, left panel and Supplemental Figure 4). The low final germination rate indicated that there might be defects in seed and/or seedling developmental processes for both Pelota and Hbs1 null mutants, which might be due to abnormally high levels of CTRD of the mRNAs regulating the relevant processes in these mutant backgrounds.

We then went on to assess if these mutant plants also have phenotypes different from those of wild-type plants when grown under stress conditions. Specifically, we wanted to determine whether these null mutants grow differently under high light conditions compared to wild-type plants given that GO terms related to light response are highly enriched in the CTRD mRNAs specific to the mutants. To answer this question, we germinated the four null mutants as well as wild-type plants under high light intensity (400 umol/m^2/s^{-1}) and again tracked their germination phenotype daily. Similar to results obtained under regular light conditions, we again observed that *pel*
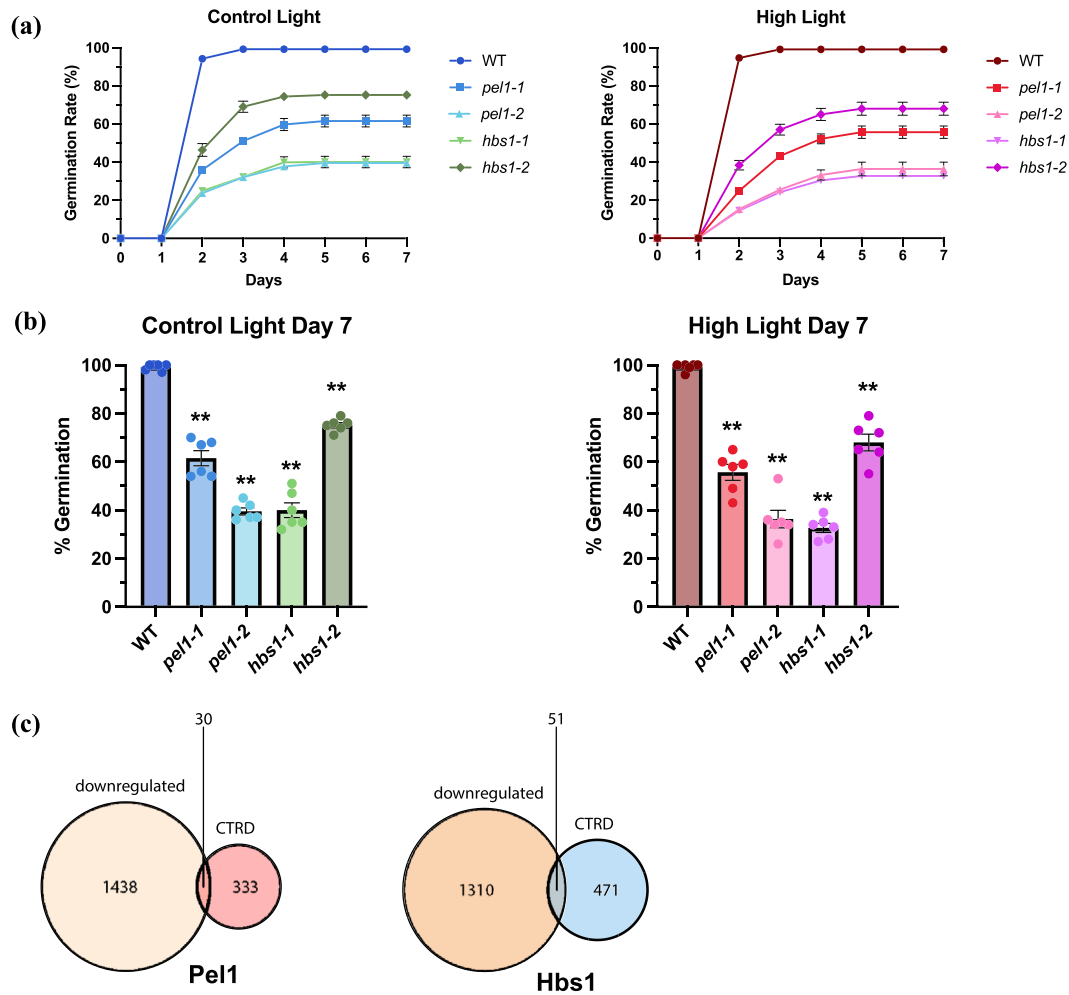
FIGURE 4 **Pelota and Hbs1 null mutants have different germination phenotypes compared to wild type plants in normal and high light conditions.** (a) Germination rate of Pelota (*pel1–1* and *pel1–2*) and Hbs1 (*hbs1–1* and *hbs1–2*) null mutants germinated under control light (left panel) and high light (right panel) conditions. Error bars represent the standard error for the mean of six biological replicates, each with at least 61 seeds per genotype. (b) Percent germination of Pelota (*pel1–1* and *pel1–2*) and Hbs1 (*hbs1–1* and *hbs1–2*) null mutants at day seven from the graph in **a)**. ** denotes p-values ≤ .01 as determined by Mann–Whitney U test. (c) The overlap between down-regulated transcripts and the transcripts undergoing CTRD in *pel* (left panel) and *hbs1* (right panel) null mutants. "Down-regulated" denotes the down-regulated transcripts identified from mRNA-seq data while "CTRD" denotes the transcripts undergoing co-translational mRNA decay.

and *hbs1* null mutants germinated at significantly (all p-values < .01; Mann–Whitney U test) lower levels as compared to wild-type under high light intensity conditions. Specifically, the germination rate of *pel1–1*, *pel1–2*, *hbs1–1*, and *hbs1–2* were 56%, 36%, 33%, and 68%, respectively, at day seven (Figure 4a,b, right panel and Supplemental Figure 5). Interestingly, the germination rates of the null mutants were slightly lower under high light intensity compared to under normal light levels, suggesting that the null mutants respond even more severely to the adverse growth conditions as compared to wild-type plants. Taken together, these results revealed that *pel* and *hbs1*, in which the co-translational decay suppression for many mRNAs involved in certain development processes and stress response is absent, have lower germination rates compared to wild-type plants, implying that co-translational mRNA decay likely plays important roles in physiological processes including seed or seedling development in Arabidopsis.

As we discovered that mis-regulated CTRD resulted in deleterious physiological outcomes, we wondered how abnormal CTRD levels disrupt normal physiological processes such as germination in Arabidopsis. Since the outcome of co-translational mRNA decay is the removal of a specific transcript, we speculated that increased CTRD levels of a certain mRNA species result in lower steady-state levels of this specific mRNA species in the cell, which could further affect certain physiological processes that the protein encoded by that mRNA is involved in. To test this hypothesis, we constructed mRNA-seq libraries in duplicates for both the wild-type plants and the mutants (*pel1–1* and *hbs1–1*) grown under regular light conditions. The libraries were sequenced with all generating ∼20–26 million mapped reads per library (Supplemental Table 2). The libraries from the biological replicates of each distinct genotype clustered together (Supplemental Figure 2B), indicating the high quality and reproducibility of these libraries. The significantly down-regulated transcripts identified from

the mRNA-seq data were then overlapped with the CTRD mRNAs specific to the mutants. Surprisingly, in both of the mutants, there is less than 10% overlap between the CTRD mRNAs and those that were down-regulated. Specifically, among the 363 CTRD mRNAs specific to *pel1–1*, 30 are significantly down-regulated (Figure 4c, left panel). Out of the 522 CTRD mRNAs specific to *hbs1–1*, 51 are significantly down-regulated (Figure 4c, right panel).

Within these down-regulated CTRD mRNAs specific to each of the mutants, we found that many of these mRNAs such as *HSP70* encode proteins that are crucial in various stress responses for both of the mutants (Berka et al., 2022; Wang et al., 2021) (Supplemental Figures 6A and 7A). We also found several developmental process-related mRNAs such as *DEK1* and *RopGEF7* for *pel1* and *hbs1*, respectively (Supplemental Figures 6B, 6C, 7B, and 7C). In total, these results demonstrated that excessive CTRD can result in a decrease in the steady state level of some transcripts, which could in turn affect the physiological processes that the proteins encoded by the transcripts are involved in and result in different phenotypes in the mutants compared to wild type plants.

Interestingly, it was previously reported that Pelota is involved in suppressing the accumulation of illegitimate siRNAs from many mRNAs (Vigh et al., 2022). Therefore, we wondered if the phenotypes observed in *pel1* mutant plants are attributable to accumulated illegitimate siRNAs. We reasoned that if the germination phenotype is related to illegitimate siRNAs, the mRNAs which the illegitimate siRNAs are generated from will be enriched in embryonic developmental or germination-related processes. By conducting Gene Ontology analysis on the mRNAs that the illegitimate siRNAs are derived from, we found that the majority of these mRNAs are responsible for developmental processes in the later stages such as leaf development and flower development rather than early-stage development (Supplemental Figure 8). Therefore, the germination phenotypes observed in Pelota null mutants are unlikely to be related to illegitimate siRNA accumulation.

3 | DISCUSSION

Since the discovery of CTRD in yeast, this novel mRNA decay mechanism has been confirmed to exist in multiple species (Guo et al., 2023; Hou et al., 2016; Ibrahim et al., 2018; Pelechano et al., 2015; Yu et al., 2016). However, the regulation as well as the physiological role of this novel decay mechanism has not been comprehensively studied to date. By re-analyzing the level of CTRD and the translation efficiency calculated from publicly available degradome sequencing datasets and their matching polysome profiling or ribosome footprinting datasets and mRNA-seq datasets, we found that highly translated mRNAs generally have low co-translational decay levels in Arabidopsis (Figure 1). It is worth noting that the dataset generated using 25-day-old seedlings has been the only outlier among all five datasets interrogated in this study. In this specific dataset, there is no significant difference in co-translational decay level between highly translated mRNAs and lowly translated mRNAs (Figure 1a, bottom right

panel). While this different trend might simply be dataset-specific, it could also imply a difference between various growth stages of Arabidopsis in the relationship between mRNA translation efficiency and the level of CTRD. However, more datasets need be analyzed in order to determine whether the difference observed in the 25-day-old seedlings dataset is truly dataset-specific or if the co-translational decay level of the transcripts in 25-day-old seedlings is truly not related to their translation level. Interestingly, it was previously discovered in yeast that the translation level is not related to the co-translational decay level (Pelechano et al., 2015). We believe that this could be an indication that whether CTRD is related to translation level is kingdom-specific. Again, more datasets from other species (including yeast) need to be analyzed to determine if this difference is truly kingdom-specific.

Given the relationship between CTRD and translation level, we then wondered if the factors that are related to impact ribosome behavior can also regulate this decay pathway since ribosome behavior is directly related to translation level. Using GMUCT, we discovered that Arabidopsis Pelota and Hbs1 are suppressors for CTRD in vivo, with Hbs1 being the stronger suppressor among the two factors (Figure 2). Future experiments can focus on determining the mechanism by which Pelota and Hbs1 suppress this decay pathway. Interestingly, the Arabidopsis Pelota and Hbs1 coding sequences have diverged significantly between yeast and multi-cellular metazoans (Kong et al., 2021; Zhang et al., 2018), suggesting that Arabidopsis and human Pelota and Hbs1 possibly gained new functions through this sequence divergence. Therefore, it will be interesting to experiment with the difference in the domains of these two factors can contribute to CTRD suppression. It is also worth looking into if there are any other factors facilitating the suppression of this degradation pathway.

From our gene ontology (GO) analyses of the co-translational decay suppression targets of Pelota and Hbs1, we found that the targets of each of the suppressors are involved in producing proteins that function in a wide range of stress and developmentally related processes (Figure 3), suggesting that the suppression of CTRD by Pelota and Hbs1 might be important for normal physiological functions in various biological processes. Interestingly, in addition to Arabidopsis, Pelota orthologs have been identified via sequence alignments in other angiosperms such as *Oryza sativa*, *Zea mays*, and *Medicago truncatula* (Zhang et al., 2018). Thus, it is worth exploring if Pelota is also able to suppress co-translational mRNA decay in these plant species, given that recent findings have revealed this decay pathway functioning in these plant species (Guo et al., 2023).

Finally, we compared the phenotypes of Pelota and Hbs1 null mutants with those of wild-type plants under regular growth conditions and found that both Pelota and Hbs1 null mutants have lower germination rates (Figure 4a,b and Supplemental Figures 4 and 5). The same was true when comparing the null mutants' germination rates to those of wild-type plants in the context of high-light treatments (Figure 4a,b and Supplemental Figures 4 and 5). As indicated in the GO analysis, both the Pelota and Hbs1 co-translational decay suppression targets are enriched with mRNAs responsible for early-stage

developmental processes (Figure 3). Additionally, we have also determined that the phenotypes are unlikely to be related to illegitimate siRNA accumulation in these mutant plants since the illegitimate siRNAs are mainly processed from mRNAs encoding proteins responsible for later stages of development rather than embryonic development (compare Figure 3 to Supplemental Figure 8). The observed low germination rates in *pel1* and *hbs1* mutants in both tested conditions provide an intriguing link between specific development-related transcripts that are affected by elevated levels of CTRD in the null mutant backgrounds and specific plant phenotypes (Supplemental Figures 6 and 7). Thus, these findings provide evidence that these targets are likely important CTRD regulatory targets of Pelota and Hbs1 that are physiologically relevant in a developmental context. This hypothesis needs to be further explored in future research projects.

Aiming at further understanding how CTRD might have resulted in the observed phenotypes, we constructed and analyzed the mRNA-seq libraries for the null mutants and wild-type plants. We found that less than 10% of the CTRD mRNAs specific to each mutant are actually down-regulated according to the mRNA-seq libraries. Among those down-regulated CTRD mRNAs, we identified many transcripts that could potentially contribute to the lower germination rate in Pelota and Hbs1 null mutants. For instance, *DEK1* (*AT1G55350*) found in the 30 down-regulated co-translationally decayed mRNAs specific to *pel* is required for endosperm and embryo development (Figures 4c, Supplemental Figure 6B, and Supplemental Figure 7B). Knocking out *DEK1* can result in embryo or endosperm development failure (Lid et al., 2005). Relatedly, *RopGEF7* (*AT5G02010*) found in the list of 51 transcripts down-regulated co-translationally decayed mRNAs specific to *hbs1* (Figure 4c, Supplemental Figure 6C, and Supplemental Figure 7C) is also related to embryo development as embryo patterning was defective in *RopGEF7* knocking down plants (Chen et al., 2011). Given that *DEK1* and *RopGEF7* are crucial for embryo development, it is very possible that the decreased quantity of *DEK1* in the Pelota null mutant and *RopGEF7* in Hbs1 null mutants caused by excessive CTRD impacted the development of embryos in these two mutants, which further resulted in defective seeds and thus lower germination rate of the mutants (Figure 4a,b and Supplemental Figures 4 and 5). However, more experiments are needed to test this hypothesis.

Interestingly, we also found that 26 and 42 of co-translationally decayed mRNAs in *pel* and *hbs1* null mutants, respectively, are upregulated (Supplemental Figure 3B,C). As mRNA concentration is determined by the velocity of both transcription and decay, we believe that these upregulated co-translationally decayed mRNAs, which represent less than 10% of the co-translationally decayed mRNAs specific to mutants, might be due to increasing transcription of these specific mRNAs overpowering the effect of co-translational decay.

The GO analyses also revealed that the CTRD suppression targets in both *pel* and *hbs1* null mutants are enriched in mRNAs responsible for light response, the exacerbated difference in germination rate between the mutants and the wild-type plants in high light conditions was another phenotype we observed for these mutant backgrounds (Figure 4b). Given that the germination rate of the wild-type plants

was not strongly influenced by the high light intensity (Figure 4a,b), this provides further evidence that this stress-related phenotype further demonstrates the lack of adaptability of these mutant backgrounds as compared wild type plants, likely due to loss of CTRD suppression. Thus, future experiments will be needed to determine the direct links between the germination phenotypes of *pel* and *hbs1* mutants and CTRD.

Taken together, these phenotypes suggest that abnormally elevated co-translational decay can lead to severe physiological defects in Arabidopsis. While we discovered that less than 10% of the mRNAs whose co-translational decay levels were elevated have decreased steady-state mRNA levels, it will be interesting to explore how the rest of the co-translational decayed mRNAs are affected by this decay mechanism. We also noticed that over 50% of analyzed GO terms for co-translational decay targets overlapped between the two null mutants (Supplemental Figure 3A), meaning that the suppression targets of Pelota and those of Hbs1 are responsible for similar processes. Thus, it will also be interesting to see if Pelota and Hbs1 double mutants have more severe phenotypes compared to single mutants under the same conditions.

In total, our study revealed that the co-translational decay level of mRNAs is inversely related to their translation level in Arabidopsis, which provides insights into further studying the regulation of this pathway in plants. For the first time, we also demonstrated that Arabidopsis Pelota and Hbs1 are suppressors of CTRD *in planta*, and their null mutants have lower germination rates under both normal growth conditions and in response to high light intensities, which provides evidence for the physiological importance of CTRD in plants. Overall, significant future research effort needs to be focused on further elucidating the mechanisms and regulatory importance of CTRD in plant transcriptomes and the physiological relevance of this decay pathway in metazoans.

4 | MATERIALS AND METHODS

4.1 | Plant materials and growth conditions

Arabidopsis thaliana ecotype Columbia (Col-0) was used in all of the studies presented herein. Mutant lines *pel1–1* (SALK_124403C), *pel1–2* (SALK_044101), *hbs1–1* (CS857798), and *hbs1–2* (SALK_141373C) were obtained from Arabidopsis Biological Resources Center (ABRC) (Alonso et al., 2003). Among these mutant lines, *pel1–1*, *hbs1–1*, and *hbs1–2* have been described in previous studies (Ge et al., 2023; Kong et al., 2021; Szádeczky-Kardoss et al., 2018, 2018). All seeds were stratified for three days at 4 °C prior to sowing. Plants were grown at 22 °C under a long-day photoperiod under ~150 μmol/m^2/s^{-1} white light. For library construction, 12-day-old seedlings grown on 1/2X Murashige and Skoog plates with 1% agar were used.

For germination assays, seed batches of wild-type and mutant plants were collected from parents that were co-cultivated at the same time under the exact same conditions described above. Seed batches were also stored in the exact same conditions after being

harvested concurrently. Both wild-type and mutant seeds were grown on .5x Murashige and Skoog plates with 1% agar. The plates were set up as in Yu et al. (Yu et al., 2017). For regular light conditions, plates were grown under ∼150 μmol/m^2/s^{-1} white light, while for high light conditions, plates were grown under ∼400 μmol/m^2/s^{-1} white light, and the temperature was kept at 22 °C.

4.2 | GMUCT and mRNA-seq library construction

Total RNA was first subjected to two rounds of polyA$^+$ selection as described previously (Willmann et al., 2014). The polyA$^+$ mRNA was then separated into two portions for GMUCT libraries and mRNA-seq libraries. The GMUCT libraries were constructed as described previously (Willmann et al., 2014). Briefly, the polyA$^+$ RNA was directly ligated with a 5' RNA adapter to capture the 5′ monophosphate-bearing degradation intermediates. The products were then subjected to another round of polyA$^+$ selection in order to remove the unligated 5′ adapter sequences. Next, the 5′ adapter-ligated mRNA fragments were reverse transcribed with random hexamers with a 3' Illumina sequencing adapter on its 5′ end. After that, the library indexes were added while the libraries are amplified by limited rounds of PCR. Finally, the products were purified using 6% TBE polyacrylamide gels in order to remove any adapter-adapter clones.

The mRNA-seq libraries were constructed as previously described (Li et al., 2012). Briefly, the polyA$^+$ mRNA was first fragmented, purified by 15% TBE-Urea polyacrylamide gel, then subjected to 5′ phosphorylation before adaptors were ligated. These products were gel purified again to remove the adaptor-adaptor clones and then PCR amplified. The PCR product was further purified using a 6% TBE polyacrylamide gel.

4.3 | GMUCT, mRNA-seq, and polysome sequencing data processing

For all the sequencing data, adaptors were trimmed using Cutadapt with default parameters (Martin, 2011). The trimmed reads were mapped to the mature mRNA sequences (primary isoforms according to available annotations) using the STAR tool with the parameters "--outFilterMultimapNmax 1 --outFilterMismatchNmax 1 --outFilterMismatchNoverLmax 0.10" (Dobin et al., 2013). For GMUCT data, the SAM files were further converted to BED files containing only the 5′ most nucleotide of each read, denoting the 5' P intermediates. The 5' P read ends overlapping with the 100 nt regions flanking stop codons were calculated using BEDTools (Quinlan & Hall, 2010). All reads were normalized to reads per million (RPM). For mRNA-seq and polysome-seq data, reads mapped to CDSs of mature mRNA sequences were counted by HT-Seq counts (Anders et al., 2015). The significantly down-regulated mRNAs were identified using DESeq2 (Love et al., 2014). The mRNAs with log$_2$ fold changes smaller than −.58 and adjusted p-values lower than .05 were considered significantly down-regulated.

4.4 | Terminal stalling index (TSI) and co-translational RNA decay index (CRI) calculations

The TSI values for co-translationally decayed mRNAs were calculated as previously described (Guo et al., 2023). Briefly, the stop codon coordinates of the main open reading frames (ORF) were first acquired from the TAIR10 annotation. The overlap between mapped 5' P read ends and the flanking 100 nt of the stop codons of main ORFs was identified using Bedtools (Quinlan & Hall, 2010). The terminal stalling index (TSI) was calculated as follows:

$$\text{Terminal Stalling Index} = \frac{\frac{5'P \text{ read ends}_{-17\,nt} + 5'P \text{ read ends}_{-16\,nt}}{2}}{\text{average } 5'P \text{ read ends of flanking } 100\,nt}$$

The −17 and −16 refer to 17 and 16 nt upstream of the first nucleotide of the stop codon, respectively. Both of the two sites are considered the 5′ ribosome boundary of translation termination sites.

The CRI was defined as previously described and calculated as follows (Yu et al., 2016):

$$\text{Co-translational RNA Decay Index} = \log_2 \frac{\frac{f_1 + f_2}{2}}{f_0}$$

f_0 here refers to the total 5' P read ends of the un-cleaved frame, where as f_1 and f_2 refer to the cleaved frames.

4.5 | Translation efficiency calculation

The translation efficiency was calculated using the same principle as in the previous studies (Ingolia et al., 2009). Reads mapped to CDSs were normalized to reads per million (RPM). Translation efficiency was calculated as RPM$_{\text{polysome-seq}}$/RPM$_{\text{mRNA-seq}}$. Note that the normalized counts for Ribo-seq datasets were directly retrieved from the count table provided by the authors (Liu et al., 2013).

4.6 | Gene ontology (GO) enrichment analysis

The gene ontology analysis was performed using agriGO v2.0 (http://systemsbiology.cau.edu.cn/agriGOv2/). The GO terms with adjusted p-values (Yekutieli method) lower than .05 and belonging to the biological process category were used for further analyses.

AUTHOR CONTRIBUTIONS
R.G. and B.D.G. conceived the study, designed the experiments, and wrote the manuscript. R.G. performed all the experiments and analyzed the data.

CONFLICT OF INTEREST STATEMENT

The Authors did not report any conflict of interest.

PEER REVIEW

The peer review history for this article is available in the Supporting Information for this article.

DATA AVAILABILITY STATEMENT

Sequencing data associated with the mRNA-seq and GMUCT libraries have been deposited in GEO (GEO: GSE247330).

ORCID

Brian D. Gregory https://orcid.org/0000-0001-7532-0138

REFERENCES

Addo-Quaye, C., Eshoo, T. W., Bartel, D. P., & Axtell, M. J. (2008). Endogenous siRNA and miRNA targets identified by sequencing of the Arabidopsis degradome. *Current Biology*, *18*, 758–762. https://doi.org/10.1016/j.cub.2008.04.042

Alonso, J. M., Stepanova, A. N., Leisse, T. J., Kim, C. J., Chen, H., Shinn, P., Stevenson, D. K., Zimmerman, J., Barajas, P., Cheuk, R., Gadrinab, C., Heller, C., Jeske, A., Koesema, E., Meyers, C. C., Parker, H., Prednis, L., Ansari, Y., Choy, N., ... Ecker, J. R. (2003). Genome-wide insertional mutagenesis of Arabidopsis thaliana. *Science*, *301*, 653–657. https://doi.org/10.1126/science.1086391

Anders, S., Pyl, P. T., & Huber, W. (2015). HTSeq--a python framework to work with high-throughput sequencing data. *Bioinformatics*, *31*, 166–169. https://doi.org/10.1093/bioinformatics/btu638

Arava, Y., Wang, Y., Storey, J. D., Liu, C. L., Brown, P. O., & Herschlag, D. (2003). Genome-wide analysis of mRNA translation profiles in Saccharomyces cerevisiae. *Proceedings of the National Academy of Sciences of the United States of America*, *100*, 3889–3894. https://doi.org/10.1073/pnas.0635171100

Belostotsky, D. A., & Sieburth, L. E. (2009). Kill the messenger: MRNA decay and plant development. *Current Opinion in Plant Biology*, *12*, 96–102. https://doi.org/10.1016/j.pbi.2008.09.003

Berka, M., Kopecká, R., Berková, V., Brzobohatý, B., & Černý, M. (2022). Regulation of heat shock proteins 70 and their role in plant immunity. *Journal of Experimental Botany*, *73*, 1894–1909. https://doi.org/10.1093/jxb/erab549

Carpentier, M. C., Deragon, J. M., Jean, V., Be, S. H. V., Bousquet-Antonelli, C., & Merret, R. (2020). Monitoring of XRN4 targets reveals the importance of Cotranslational decay during Arabidopsis development. *Plant Physiology*, *184*, 1251–1262. https://doi.org/10.1104/pp.20.00942

Chen, M., Liu, H., Kong, J., Yang, Y., Zhang, N., Li, R., Yue, J., Huang, J., Li, C., Cheung, A. Y., & Tao, L. Z. (2011). RopGEF7 regulates PLETHORA-dependent maintenance of the root stem cell niche in Arabidopsis. *Plant Cell*, *23*, 2880–2894. https://doi.org/10.1105/tpc.111.085514

Dermit, M., Dodel, M., & Mardakheh, F. K. (2017). Methods for monitoring and measurement of protein translation in time and space. *Molecular BioSystems*, *13*, 2477–2488. https://doi.org/10.1039/C7MB00476A

Dobin, A., Davis, C. A., Schlesinger, F., Drenkow, J., Zaleski, C., Jha, S., Batut, P., Chaisson, M., & Gingeras, T. R. (2013). STAR: Ultrafast universal RNA-seq aligner. *Bioinformatics*, *29*, 15–21. https://doi.org/10.1093/bioinformatics/bts635

Finch-Savage, W. E., & Leubner-Metzger, G. (2006). Seed dormancy and the control of germination. *The New Phytologist*, *171*, 501–523. https://doi.org/10.1111/j.1469-8137.2006.01787.x

Ge, L., Cao, B., Qiao, R., Cui, H., Li, S., Shan, H., Gong, P., Zhang, M., Li, H., Wang, A., Zhou, X., & Li, F. (2023). SUMOylation-modified Pelota-Hbs1 RNA surveillance complex restricts the infection of potyvirids in plants. *Molecular Plant*, *16*, 632–642. https://doi.org/10.1016/j.molp.2022.12.024

German, M. A., Luo, S., Schroth, G., Meyers, B. C., & Green, P. J. (2009). Construction of parallel analysis of RNA ends (PARE) libraries for the study of cleaved miRNA targets and the RNA degradome. *Nature Protocols*, *4*, 356–362. https://doi.org/10.1038/nprot.2009.8

Gregory, B. D., O'Malley, R. C., Lister, R., Urich, M. A., Tonti-Filippini, J., Chen, H., Millar, A. H., & Ecker, J. R. (2008). A link between RNA metabolism and silencing affecting Arabidopsis development. *Developmental Cell*, *14*, 854–866. https://doi.org/10.1016/j.devcel.2008.04.005

Guo, R., Yu, X., & Gregory, B. D. (2023). The identification of conserved sequence features of co-translationally decayed mRNAs and upstream open reading frames in angiosperm transcriptomes. *Plant Direct*, *7*, e479. https://doi.org/10.1002/pld3.479

Guydosh, N. R., & Green, R. (2014). Dom34 rescues ribosomes in 3′ untranslated regions. *Cell*, *156*, 950–962. https://doi.org/10.1016/j.cell.2014.02.006

Heck, A. M., & Wilusz, J. (2018). The interplay between the RNA decay and translation machinery in eukaryotes. *Cold Spring Harbor Perspectives in Biology*, *10*, a032839. https://doi.org/10.1101/cshperspect.a032839

Hilal, T., Yamamoto, H., Loerke, J., Bürger, J., Mielke, T., & Spahn, C. M. (2016). Structural insights into ribosomal rescue by Dom34 and Hbs1 at near-atomic resolution. *Nature Communications*, *7*, 13521. https://doi.org/10.1038/ncomms13521

Hou, C. Y., Lee, W. C., Chou, H. C., Chen, A. P., Chou, S. J., & Chen, H. M. (2016). Global analysis of truncated RNA ends reveals new insights into ribosome stalling in plants. *Plant Cell*, *28*, 2398–2416. https://doi.org/10.1105/tpc.16.00295

Hu, W., Petzold, C., Coller, J., & Baker, K. E. (2010). Nonsense-mediated mRNA decapping occurs on polyribosomes in Saccharomyces cerevisiae. *Nature Structural & Molecular Biology*, *17*, 244–247. https://doi.org/10.1038/nsmb.1734

Hu, W., Sweet, T. J., Chamnongpol, S., Baker, K. E., & Coller, J. (2009). Co-translational mRNA decay in Saccharomyces cerevisiae. *Nature*, *461*, 225–229. https://doi.org/10.1038/nature08265

Ibrahim, F., Maragkakis, M., Alexiou, P., & Mourelatos, Z. (2018). Ribothrypsis, a novel process of canonical mRNA decay, mediates ribosome-phased mRNA endonucleolysis. *Nature Structural & Molecular Biology*, *25*, 302–310. https://doi.org/10.1038/s41594-018-0042-8

Ingolia, N. T., Ghaemmaghami, S., Newman, J. R., & Weissman, J. S. (2009). Genome-wide analysis in vivo of translation with nucleotide resolution using ribosome profiling. *Science*, *324*, 218–223. https://doi.org/10.1126/science.1168978

Karginov, F. V., & Hannon, G. J. (2013). Remodeling of Ago2-mRNA interactions upon cellular stress reflects miRNA complementarity and correlates with altered translation rates. *Genes & Development*, *27*, 1624–1632. https://doi.org/10.1101/gad.215939.113

Kong, W., Tan, S., Zhao, Q., Lin, D. L., Xu, Z. H., Friml, J., & Xue, H. W. (2021). mRNA surveillance complex PELOTA-HBS1 regulates phosphoinositide-dependent protein kinase1 and plant growth. *Plant*

Physiology, *186*, 2003–2020. https://doi.org/10.1093/plphys/kiab199

Li, F., Zheng, Q., Ryvkin, P., Dragomir, I., Desai, Y., Aiyer, S., Valladares, O., Yang, J., Bambina, S., Sabin, L. R., Murray, J. I., Lamitina, T., Raj, A., Cherry, S., Wang, L. S., & Gregory, B. D. (2012). Global analysis of RNA secondary structure in two metazoans. *Cell Reports*, *1*, 69–82. https://doi.org/10.1016/j.celrep.2011.10.002

Lid, S. E., Olsen, L., Nestestog, R., Aukerman, M., Brown, R. C., Lemmon, B., Mucha, M., Opsahl-Sorteberg, H. G., & Olsen, O. A. (2005). Mutation in the Arabidopisis thaliana DEK1 calpain gene perturbs endosperm and embryo development while over-expression affects organ development globally. *Planta*, *221*, 339–351. https://doi.org/10.1007/s00425-004-1448-6

Lin, Z., Gasic, I., Chandrasekaran, V., Peters, N., Shao, S., Mitchison, T. J., & Hegde, R. S. (2020). TTC5 mediates autoregulation of tubulin via mRNA degradation. *Science*, *367*, 100–104. https://doi.org/10.1126/science.aaz4352

Lin, M. C., Tsai, H. L., Lim, S. L., Jeng, S. T., & Wu, S. H. (2017). Unraveling multifaceted contributions of small regulatory RNAs to photomorphogenic development in Arabidopsis. *BMC Genomics*, *18*, 559. https://doi.org/10.1186/s12864-017-3937-6

Liu, M. J., Wu, S. H., Wu, J. F., Lin, W. D., Wu, Y. C., Tsai, T. Y., Tsai, H. L., & Wu, S. H. (2013). Translational landscape of photomorphogenic Arabidopsis. *Plant Cell*, *25*, 3699–3710. https://doi.org/10.1105/tpc.113.114769

Love, M. I., Huber, W., & Anders, S. (2014). Moderated estimation of fold change and dispersion for RNA-seq data with DESeq2. *Genome Biology*, *15*, 550. https://doi.org/10.1186/s13059-014-0550-8

Martin, M. (2011). Cutadapt removes adapter sequences from high-throughput sequencing reads. *Embnet Journal*, *2011*(17), 3. https://doi.org/10.14806/ej.17.1.200

Nagarajan, V. K., Jones, C. I., Newbury, S. F., & Green, P. J. (2013). XRN 5′→3′ exoribonucleases: Structure, mechanisms and functions. *Biochimica et Biophysica Acta*, *1829*, 590–603. https://doi.org/10.1016/j.bbagrm.2013.03.005

Park, J. H., & Shin, C. (2014). MicroRNA-directed cleavage of targets: Mechanism and experimental approaches. *BMB Reports*, *47*, 417–423. https://doi.org/10.5483/BMBRep.2014.47.8.109

Parker, R. (2012). RNA degradation in saccharomyces cerevisae. *Genetics*, *191*, 671–702. https://doi.org/10.1534/genetics.111.137265

Pelechano, V., Wei, W., & Steinmetz, L. M. (2015). Widespread co-translational RNA decay reveals ribosome dynamics. *Cell*, *161*, 1400–1412. https://doi.org/10.1016/j.cell.2015.05.008

Piccirillo, C. A., Bjur, E., Topisirovic, I., Sonenberg, N., & Larsson, O. (2014). Translational control of immune responses: From transcripts to translatomes. *Nature Immunology*, *15*, 503–511. https://doi.org/10.1038/ni.2891

Pisareva, V. P., Skabkin, M. A., Hellen, C. U., Pestova, T. V., & Pisarev, A. V. (2011). Dissociation by Pelota, Hbs1 and ABCE1 of mammalian vacant 80S ribosomes and stalled elongation complexes. *The EMBO Journal*, *30*, 1804–1817. https://doi.org/10.1038/emboj.2011.93

Quinlan, A. R., & Hall, I. M. (2010). BEDTools: A flexible suite of utilities for comparing genomic features. *Bioinformatics*, *26*, 841–842. https://doi.org/10.1093/bioinformatics/btq033

Steinbrecher, T., & Leubner-Metzger, G. (2017). The biomechanics of seed germination. *Journal of Experimental Botany*, *68*, 765–783. https://doi.org/10.1093/jxb/erw428

Szádeczky-Kardoss, I., Csorba, T., Auber, A., Schamberger, A., Nyikó, T., Taller, J., Orbán, T. I., Burgyán, J., & Silhavy, D. (2018). The nonstop decay and the RNA silencing systems operate cooperatively in plants. *Nucleic Acids Research*, *46*, 4632–4648. https://doi.org/10.1093/nar/gky279

Szádeczky-Kardoss, I., Gál, L., Auber, A., Taller, J., & Silhavy, D. (2018). The no-go decay system degrades plant mRNAs that contain a long A-stretch in the coding region. *Plant Science*, *275*, 19–27. https://doi.org/10.1016/j.plantsci.2018.07.008

Tian, T., Liu, Y., Yan, H., You, Q., Yi, X., Du, Z., Xu, W., & Su, Z. (2017). agriGO v2.0: A GO analysis toolkit for the agricultural community, 2017 update. *Nucleic Acids Research*, *45*, W122–w129. https://doi.org/10.1093/nar/gkx382

Tsuboi, T., Kuroha, K., Kudo, K., Makino, S., Inoue, E., Kashima, I., & Inada, T. (2012). Dom34:hbs1 plays a general role in quality-control systems by dissociation of a stalled ribosome at the 3′ end of aberrant mRNA. *Molecular Cell*, *46*, 518–529. https://doi.org/10.1016/j.molcel.2012.03.013

Vigh, M. L., Bressendorff, S., Thieffry, A., Arribas-Hernández, L., & Brodersen, P. (2022). Nuclear and cytoplasmic RNA exosomes and PELOTA1 prevent miRNA-induced secondary siRNA production in Arabidopsis. *Nucleic Acids Research*, *50*, 1396–1415. https://doi.org/10.1093/nar/gkab1289

Wang, T. Y., Wu, J. R., Duong, N. K. T., Lu, C. A., Yeh, C. H., & Wu, S. J. (2021). HSP70-4 and farnesylated AtJ3 constitute a specific HSP70/HSP40-based chaperone machinery essential for prolonged heat stress tolerance in Arabidopsis. *Journal of Plant Physiology*, *261*, 153430. https://doi.org/10.1016/j.jplph.2021.153430

Willmann, M. R., Berkowitz, N. D., & Gregory, B. D. (2014). Improved genome-wide mapping of uncapped and cleaved transcripts in eukaryotes—GMUCT 2.0. *Methods*, *67*, 64–73. https://doi.org/10.1016/j.ymeth.2013.07.003

Yu, X., Willmann, M. R., Anderson, S. J., & Gregory, B. D. (2016). Genome-wide mapping of uncapped and cleaved transcripts reveals a role for the nuclear mRNA cap-binding complex in Cotranslational RNA decay in Arabidopsis. *Plant Cell*, *28*, 2385–2397. https://doi.org/10.1105/tpc.16.00456

Yu, L. H., Wu, J., Zhang, Z. S., Miao, Z. Q., Zhao, P. X., Wang, Z., & Xiang, C. B. (2017). Arabidopsis MADS-box transcription factor AGL21 acts as environmental surveillance of seed germination by regulating ABI5 expression. *Molecular Plant*, *10*, 834–845. https://doi.org/10.1016/j.molp.2017.04.004

Zhang, X. B., Feng, B. H., Wang, H. M., Xu, X., Shi, Y. F., He, Y., Chen, Z., Sathe, A. P., Shi, L., & Wu, J. L. (2018). A substitution mutation in OsPELOTA confers bacterial blight resistance by activating the salicylic acid pathway. *Journal of Integrative Plant Biology*, *60*, 160–172. https://doi.org/10.1111/jipb.12613

SUPPORTING INFORMATION

Additional supporting information can be found online in the Supporting Information section at the end of this article.